

Compression Braking Control for Heavy-Duty Vehicles¹

M. Druzhinina, L. Moklegaard and A. G. Stefanopoulou
University of California, Santa Barbara

Abstract

Modern heavy-duty vehicles are equipped with a compression braking mechanism that augments their braking capability and reduces the wear of the conventional friction brakes. In this paper we consider a vehicle speed control problem using a continuously variable compression braking mechanism. The variability of the compression brake is achieved through the control of the brake valve of the vehicle's turbocharged diesel engine. An adaptive controller is designed to ensure good speed tracking performance in brake-by-wire, or vehicle-following, driving scenarios even during large variations in mass and road grade. Our approach is to first consider the model without compression brake actuator dynamics and derive a Model Reference Adaptive Controller using the Speed-Gradient procedure. Then, the actuator dynamics are included in the design via the use of the backstepping procedure. The backstepping controller is implemented with a simplified numerical differentiator-based approximation.

1 Introduction

In Intelligent Vehicle Highway Systems (IVHS), the major goals are to increase highway capacity and to enhance driving safety by automatic longitudinal and lateral control of vehicles [1]-[3]. Modern Heavy Duty Vehicles (HDV) operate very close to the speed, acceleration and headway range of passenger vehicles. At the same time, their mass and inertia are much larger. Hence powerful acceleration/deceleration actuation is needed to enable the driver to safely merge, follow and react to traffic flow changes.

To improve the braking performance of the HDVs, additional braking mechanisms, such as a compression brake, are frequently used. In the compression braking mode the conventional gas exchange process of the turbocharged diesel engine that powers the HDV is altered and the engine is transformed into a compressor that absorbs kinetic energy from the crankshaft. During compression braking mode the fuel injection and combustion are inhibited. The kinetic energy is dissipated through the work done by the pistons to compress the air charge. The compressed air is consequently released in the exhaust manifold through a secondary opening of the exhaust valve at the end of the compression stroke. We call the secondary opening of the exhaust valve as Brake Valve Opening (BVO). Due to geometric constraints, the valve lift profile is considerably different for the exhaust and the brake events, as shown in Figure 1. In conventional compression

braking mechanisms, BVO is fixed with respect to the crank angle degrees resulting in on-off retarding mechanisms [4]. Selective activation of the BVO of a number of cylinders can provide discretely variable retarding power as in [5]. The retarding mechanism we consider here allows continuously variable retarding power through control of BVO [6]. The timing of BVO (specified in crank angle degrees) is the input signal to the compression braking mechanism and is physically limited to the range $v_{cb,min} = 620$ to $v_{cb,max} = 680$ degrees after Top Dead Center (TDC) (see Figure 1).

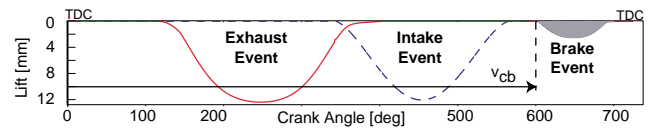


Figure 1: Lift profiles for exhaust, intake and brake events.

The variable compression brake increases the overall decelerating capability of the vehicle and can be used as the sole decelerating actuator without the assistance of friction brakes during non-aggressive maneuvers. Consequently, the application and intensity of the friction brakes can be reduced resulting in a significant decrease in the vehicle maintenance costs.

Thus, in this paper we concentrate on the longitudinal speed control problem using only variable compression braking. We consider braking control for a Class-8 HDV during operation on a descending grade with the objective to achieve vehicle speed tracking despite unknown road conditions. To ensure good speed tracking even during large variations in vehicle mass (payload) and road grade, an adaptive controller is developed.

The first results on adaptive longitudinal control design for HDV are presented in [7, 8], where the authors develop an adaptive controller for a HDV with conventional friction brakes using the direct adaptation of PIQ controller gains. In this paper, we derive a Model Reference Adaptive Controller in terms of system parameter estimates. The updates for the estimates are generated using the Speed-Gradient technique [9]. Our control design approach is to first consider the model without compression brake actuator dynamics. Then the actuator dynamics are accounted for in the controller through the use of a backstepping procedure. The backstepping controller is implemented using a numerical differentiator based approximation.

To model the effect of the novel braking actuator, namely variable compression brake, on the engine and vehicle operation, a detailed crank angle based engine model has been developed

¹This research is supported in part by the California Department of Transportation through the California PATH Program under MOU 372 and MOU 393; matching funds are provided by Mack Trucks, Inc.

in [10]. The control design in this paper is based on a reduced-order nonlinear approximation of the crankangle-based model developed in [11].

In addition to speed tracking we are also able, under additional persistence of excitation type conditions, to estimate the unknown parameters, namely vehicle mass and road grade. These estimates can be used for other purposes in Advanced Vehicle Control Systems (AVCS). As we will show, the convergence of the estimates is ensured when the desired speed value changes in a step-wise or other periodic fashion. This is typically guaranteed in urban driving cycles. If the excitation does not occur during normal driving, it has to be introduced artificially.

The paper is organized as follows. In Sections 2 and 3 we review the models for longitudinal vehicle speed and compression brake actuator dynamics and we formally state the control problem. Sensitivity of the input-output response due to variations in mass and road grade is shown in Section 4. The observed sensitivity serves as a motivation for us to pursue the adaptive control approach. In Section 5 we develop a Model Reference Adaptive Controller (MRAC) assuming instantaneous actuator response. In Section 6, we extend the control design to the case with the actuator dynamics. The controller performance is demonstrated through simulations in Section 7.

2 Vehicle Dynamics Model

Consider the vehicle operation during a driving maneuver on a descending grade with β degrees inclination ($\beta = 0$ corresponds to no inclination, $\beta < 0$ corresponds to a descending grade). It is assumed that during the descent, the engine is not fueled and is operated in the compression braking mode.

A lumped parameter model approximation is used to describe the vehicle longitudinal dynamics during compression braking. For fixed gear operation the engine crankshaft rotational speed, ω , is expressed by:

$$J_t \dot{\omega} = T_{cb} + r_g (F_\beta - F_{qdr}) \quad (1)$$

where,

ω is the engine rotational speed, (rad/sec), related to the vehicle speed value $v = \omega r_g$, (m/sec)

$r_g = \frac{r_\omega}{g_t g_{fd}}$ is the total gear ratio, where r_ω is the wheel diameter, g_t is the transmission gear ratio, g_{fd} is the final drive gear ratio (assumed to be known constants)

$J_t = m r_g^2 + J_e$ is the total vehicle inertia reflected to the engine shaft (unknown constant, depends on the vehicle loading conditions), where J_e is the engine crankshaft inertia

m is the mass of the vehicle (unknown constant, depends on the mass of payload), (kg)

$F_{qdr} = C_q r_g^2 \omega^2$ is the quadratic resistive force (primarily, force due to aerodynamic resistance, but we also include friction resistive terms)

$C_q = \frac{C_d A \rho}{2} + C_f$ is the quadratic resistive coefficient, where C_d is the aerodynamic drag coefficient, ρ is ambient air density, A is the frontal area of the vehicle, C_f is the friction

coefficient (assumed to be known constants)

$F_\beta(m, \beta)$ is the force due to road grade (β) (assumed to be an unknown constant) and the rolling resistance of the road (μ): $F_\beta(m, \beta) = -\mu g m \cos \beta - m g \sin \beta$

T_{cb} is the shaft torque applied by the engine to the driveshaft (supposed to be negative during compression braking).

The speed control problem is to ensure that the engine rotational speed ω tracks the desired reference speed $\omega_d(t)$ as the vehicle proceeds the descending grade: $\omega \rightarrow \omega_d(t)$. This ensures that $v \rightarrow v_d(t)$ as long as the gear ratio remains constant.

Remark 1: We assume the existence of a higher level supervisory controller which selects transmission gear ratio, g_t , if a frequent saturation of BVO timing is detected. Specifically, if the limits of the compression braking torque are frequently reached, a different transmission gear ratio can be selected. With an appropriate gear selection one can effectively “size” the power due to gravity that is reflected on the engine shaft, see (1). The control scheme we develop below can be easily extended to include gear ratio optimization and selection.

Remark 2: We assume that the desired vehicle speed $\omega_d(t)$ is derived from the driver’s brake pedal position through a calibration map. These calibration maps are typically developed by skilled drivers and can be used in a brake-by-wire mode. In Automated Highway Systems (AHS) the value of $\omega_d(t)$ may be generated from a lead vehicle.

3 Brake Actuator Dynamics

In [10] we have developed a detailed crank angle based engine model that describes the engine dynamics during compression braking and transition between fueling and compression braking modes. This high-order dynamic model captures the manifold and cylinder emptying/filling dynamics and the turbocharger rotational dynamics. In [11] we show that the high-order model can be approximated by a lower-order model. Namely, the compression brake torque on the crankshaft, T_{cb} , is calculated using the following first order differential equation:

$$\dot{T}_{cb} = -\lambda_{cb}(T_{cb} - T_{st}), \quad (2)$$

where λ_{cb} is approximated with a linear function of the engine speed, $\lambda_{cb} = \eta_0 + \eta_1 \omega$. The value of λ_{cb} is implicitly limited by upper and lower limits on the engine speed. The feasible values of λ_{cb} are within the range $\lambda_{cb, min} = \lambda_{cb}(\omega_{min})$ to $\lambda_{cb, max} = \lambda_{cb}(\omega_{max})$. The steady-state braking torque, T_{st} , is a nonlinear function of the engine speed ω and the BVO timing v_{cb} :

$$T_{st}(\omega, v_{cb}) = \alpha_0 + \alpha_1 \omega + \alpha_2 v_{cb} + \alpha_3 v_{cb} \omega + \alpha_4 \omega^2. \quad (3)$$

The fact that λ_{cb} depends on ω is due to the turbocharger and manifold filling dynamics that become faster as the engine speed increases. We assume that the BVO timing can be controlled instantaneously or considerably faster than the engine dynamics in (2). Engine manufacturers are intensively pursuing the development of appropriate hardware [6]. Consequently, we assume for now that the system (2), (3) represents the dominant compression brake actuator dynamics. The

BVO timing limits translate into limits on the braking torque $T_{st,min}(\omega) = T_{st}(v_{cb,max}, \omega)$, $T_{st,max}(\omega) = T_{st}(v_{cb,min}, \omega)$.

The controller is designed directly in terms of torque T_{st} , while the corresponding value of the BVO timing v_{cb} is obtained by inverting the static torque regression (3).

4 Sensitivity Analysis

A sensitivity analysis and an evaluation of the model variations and uncertainties across operating regimes allows us to assess the difficulties in the control design. In particular, variations in the vehicle mass greatly affect the vehicle dynamics. The mass for the system can vary as much as 400 percent from a configuration of being a tractor only, to a configuration of being a tractor and one or more trailers. Figure 2 demonstrates the differences in the linearized open loop system frequency response for different values of the vehicle mass. Similar trends can be ascertained for the road grade and gear ratio variations. Clearly, adaptation is needed to ensure that the vehicle response remains the same irrespective of these parameter variations.

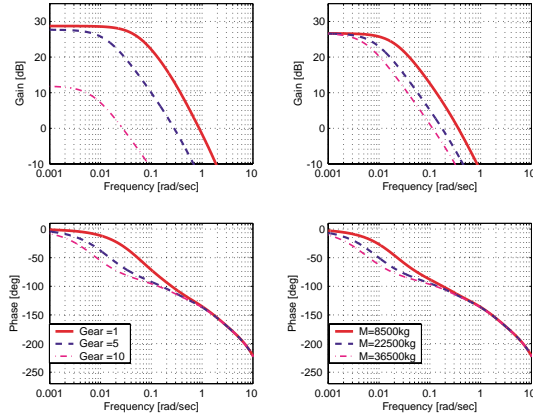


Figure 2: Frequency response of the transfer function from Δv_{cb} to $\Delta\omega$ for various values of the vehicle mass and gear ratio. This plot is from [10] where additional dynamics were introduced by a BVO hydraulic mechanism (not treated here).

5 Model Reference Adaptive Controller

In this section we develop a Model Reference Adaptive Controller (MRAC) which ensures the vehicle speed tracking during braking irrespective of variations in vehicle mass and road grade. The design of the controller algorithm is first done for the case without the actuator dynamics. In Section 6 we extend the controller algorithm to account for the actuator dynamics.

Let us assume that the mass m of the vehicle (which depends on the mass of payload) is an unknown constant. This implies that the total vehicle inertia $J_t(m)$ is an unknown constant as long as the gear ratio remains fixed. Moreover, assume that the road grade β (i.e. the hill inclination angle) is an unknown constant, which implies that the force $F_\beta(m, \beta)$ due to road grade (β) and the rolling resistance of the road (μ) is an unknown constant as well. Then the vehicle model (1) in the

parametric form is

$$\dot{\omega} = \theta_1^{-1}(u - r_g^3 C_a \omega^2 + \theta_2), \quad (4)$$

where u is the shaft torque T_{cb} , and θ_1 , θ_2 are unknown parameters. In particular, $\theta_1 = J_t > 0$, $\theta_2 = r_g F_\beta$.

Remark: Note that the sign of θ_1 which is the total vehicle inertia is always positive. This property is critical to being able to develop a MRAC design.

To design MRAC we introduce a reference model that captures the desired closed-loop behavior. Specifically,

$$\dot{\omega}_m = -\lambda\omega_m + \lambda\omega_d, \quad (5)$$

where $\omega_d(t)$ is the desired vehicle speed and $\lambda > 0$ controls the speed of response, whereby larger values of λ correspond to faster responses.

Denoting the tracking error by $e = \omega - \omega_m$, we obtain:

$$\dot{e} = \theta_1^{-1}(u - r_g^3 C_a \omega^2 + \theta_2) + \lambda\omega_m - \lambda\omega_d. \quad (6)$$

Using the certainty equivalence principle, if θ_1 , θ_2 were known we would define the feedback law as follows:

$$u = r_g^3 C_a \omega^2 - \theta_2 + \theta_1 \lambda (\omega - \omega_d). \quad (7)$$

If θ_1 , θ_2 were known, this controller would guarantee $e(t) \rightarrow 0$. Since the parameters are unknown, we replace them by their estimates, $\hat{\theta}_1$, $\hat{\theta}_2$ in the control law (7):

$$u = r_g^3 C_a \omega^2 - \hat{\theta}_2 - \hat{\theta}_1 \lambda (\omega - \omega_d). \quad (8)$$

The parameters $\hat{\theta}_1$, $\hat{\theta}_2$ will be adjusted by the adaptation law. The error model is given by:

$$\dot{e} = -\lambda e + \theta_1^{-1} \lambda (\omega - \omega_d) (\theta_1 - \hat{\theta}_1) + \theta_1^{-1} (\theta_2 - \hat{\theta}_2). \quad (9)$$

The update laws are obtained using the Speed Gradient methodology [9]. This is a general technique for controlling nonlinear systems through an appropriate selection and minimization of a goal function. The controller is designed to provide the decrease of the goal function along the trajectories of the system. The goal function Q is selected to address the speed tracking objective, namely $Q(e) = \frac{\theta_1}{2} e^2 \geq 0$. Note that $Q(e) > 0$ if $e \neq 0$ because $\theta_1 > 0$. Then,

$$\dot{Q} = \theta_1 e \dot{e} = -\lambda \theta_1 e^2 + e \lambda (\omega - \omega_d) (\theta_1 - \hat{\theta}_1) + e (\theta_2 - \hat{\theta}_2),$$

and in accordance with the SG approach, we calculate the derivative of \dot{Q} with respect to $\hat{\theta}_1$ and $\hat{\theta}_2$ (the gradient of the "speed") and define the following adaptation laws:

$$\dot{\hat{\theta}}_1 = -\gamma_1 \nabla_{\hat{\theta}_1} \dot{Q} = \gamma_1 e \lambda (\omega - \omega_d), \quad \gamma_1 > 0. \quad (10)$$

$$\dot{\hat{\theta}}_2 = -\gamma_2 \nabla_{\hat{\theta}_2} \dot{Q} = \gamma_2 e, \quad \gamma_2 > 0. \quad (11)$$

The stability results can be proved using the following Lyapunov function:

$$V(e, \tilde{\theta}) = Q(e) + 0.5 \gamma_1^{-1} \tilde{\theta}_1^2 + 0.5 \gamma_2^{-1} \tilde{\theta}_2^2 \geq 0, \quad (12)$$

where $\tilde{\theta} = [\tilde{\theta}_1 \ \tilde{\theta}_2]^T$, and $\tilde{\theta}_i = \theta_i - \hat{\theta}_i$, $i = 1, 2$. Calculating the time derivative of V , using the adaptation laws (10)-(11), we obtain

$$\dot{V} = \dot{Q} - \gamma_1^{-1} \tilde{\theta}_1 \dot{\hat{\theta}}_1 - \gamma_2^{-1} \tilde{\theta}_2 \dot{\hat{\theta}}_2 = -\lambda \theta_1 e^2 \leq 0.$$

The last inequality means that $V(e(t), \tilde{\theta}(t))$ is a non-increasing function of time. It implies boundedness of $V(e(t), \tilde{\theta}(t))$ and $Q(e(t))$ that, in turn, means boundedness of $e(t)$, $\tilde{\theta}(t)$ (thanks to radial unboundedness of $Q(e)$). Moreover, using the Barbalat's lemma, we can prove that $e(t) \rightarrow 0$ (i.e. $\omega \rightarrow \omega_m$). Coupled with $\omega_m \rightarrow \omega_d$, this implies that $\omega \rightarrow \omega_d(t)$, i.e. the speed tracking goal is achieved.

Remark: In the actual implementation of (10)-(11) we employ the feasible range projection whereby the updates are stopped if the parameter estimates attempt to leave the region where the parameters are known to physically lie in. This is done to improve parameter estimate transient behavior and also to ensure that the estimates always lie within a physically reasonable range.

Notice that the time derivative of the Lyapunov function depends only on $e(t)$ and does not depend on $\tilde{\theta}(t)$, i.e. the solution $e(t), \tilde{\theta}(t)$ is stable but not asymptotically stable (with respect to the whole state vector). In order to guarantee the convergence of the estimates $\hat{\theta}_1(t)$, $\hat{\theta}_2(t)$ to their true values θ_1 , θ_2 , we need to require that the vector function $R = [1 \ \lambda(\omega - \omega_d)]^T$ is persistently excited [13]. Practically, the persistent excitation condition can be satisfied if the value ω_d varies significantly (e.g., includes at least 2 sinusoids: one of the two sinusoids can be a constant function, i.e. a sinusoid with zero frequency, the other one should have a non-zero frequency). In this case, we can guarantee the identifying properties of our control algorithm, i.e. $\lim_{t \rightarrow \infty} \hat{\theta}_1 = \theta_1$, $\lim_{t \rightarrow \infty} \hat{\theta}_2 = \theta_2$. This implies that the estimates of the vehicle mass m and road grade β will tend to their true values. The simulation results which demonstrate the parameter convergence are shown in Section 7.

6 Controller Design Including Brake Actuator Dynamics

In this section, we extend the design to include the brake actuator dynamics (2). The system with the actuator dynamics is given by:

$$J_t \dot{\omega} = T_{cb} + r_g (-C_q r_g^2 \omega^2 + F_\beta) \quad (13)$$

$$\dot{T}_{cb} = -\lambda_{cb} (T_{cb} - T_{st}), \quad (14)$$

where T_{st} is now considered as a control input and λ_{cb} is a function of engine speed ω .

The higher order controller that takes the dynamics in (2) into account is designed using a backstepping approach [12]. In accordance with this iterative procedure we have to consider T_{cb} as a *virtual* input of the first-order system (13) and design a stabilizing control law $\alpha(e, \hat{\theta}_1, \hat{\theta}_2)$ and the update laws for $\hat{\theta}_1$, $\hat{\theta}_2$ for (13) as the first step. This has been done in the previous Section and

$$\alpha(e, \hat{\theta}_1, \hat{\theta}_2) = r_g^3 C_a \omega^2 - \hat{\theta}_2 - \hat{\theta}_1 \lambda(\omega - \omega_d). \quad (15)$$

The error between T_{cb} and α is denoted by z :

$$z = T_{cb} - \alpha(e, \hat{\theta}_1, \hat{\theta}_2).$$

To account for this error, we augment the Lyapunov function (12) with the term $0.5z^2$:

$$V_a(e, z, \tilde{\theta}_1, \tilde{\theta}_2) = V(e, \tilde{\theta}_1, \tilde{\theta}_2) + 0.5z^2. \quad (16)$$

The time-derivative of V_a along the trajectories of the closed-loop system (13), (14), (15), (10),(11) is given by

$$\begin{aligned} \dot{V}_a &= \theta_1 e \dot{e} - \gamma_1^{-1} \tilde{\theta}_1 \dot{\hat{\theta}}_1 - \gamma_2^{-1} \tilde{\theta}_2 \dot{\hat{\theta}}_2 + z(\dot{T}_{cb} - \dot{\alpha}) = \\ &= -\theta_1 \lambda e^2 + z(e - \lambda_{cb}(T_{cb} - T_{st}) - \dot{\alpha}) \end{aligned} \quad (17)$$

Therefore, to guarantee negative definiteness of \dot{V}_a we need to choose T_{st} to make the last term of (17) to be equal to $-kz$, where $k > 0$ is a controller gain. This is achieved with the following control law:

$$T_{st} = T_{cb} + \lambda_{cb}^{-1} (-kz - e + \dot{\alpha}) \quad (18)$$

where $\dot{\alpha} = (2C_q r_g^3) \dot{\omega} - \lambda(\omega - \omega_d) \hat{\theta}_1 - \hat{\theta}_2 + \hat{\theta}_1 \lambda \dot{\omega}_d$.

Since $z = T_{cb} - \alpha$,

$$T_{st} = (1 - k\lambda_{cb}^{-1})T_{cb} - \lambda_{cb}^{-1}(e - k\alpha - \dot{\alpha}) \quad (19)$$

Note that (18) (or (19)) depend on several quantities that we do not measure directly. In particular, we do not measure the shaft torque T_{cb} . To deal with this issue, we use an open-loop observer,

$$\dot{\hat{T}}_{cb} = -\lambda_{cb}(\hat{T}_{cb} - T_{st}),$$

and use the estimate \hat{T}_{cb} in place of T_{cb} .

Remark: In order to guarantee that $e(t) \rightarrow 0$, $z(t) \rightarrow 0$ with the observer, the gain k in (18) (or (19)) has to be selected so that $k > \lambda_{cb, \max}/4$. Indeed, define $e_{cb} = \hat{T}_{cb} - T_{cb}$. Then, $\dot{e}_{cb} = -\lambda_{cb} e_{cb}$, and $T_{st} = T_{cb} + e_{cb} + \lambda_{cb}^{-1}(-kz - e + \dot{\alpha})$. Let $V_{a1} = V_a + \frac{1}{2}e_{cb}^2$. Calculating the derivative of V_{a1}

$$\begin{aligned} \dot{V}_{a1} &= -\lambda e^2 - kz^2 + z\lambda_{cb} e_{cb} - \lambda_{cb} e_{cb}^2 = \\ &= -\lambda e^2 - (k - \lambda_{cb}/4)z^2 - \lambda_{cb}(e_{cb} - 0.5 \cdot z)^2, \end{aligned}$$

we obtain that \dot{V}_{a1} is negative definite with respect to e and z if $k > \lambda_{cb, \max}(\omega)/4 \geq \lambda_{cb}(\omega)/4$.

Note that (18) also depends on the time derivative of ω which is not measured (unless there is an accelerometer on-board). Therefore, to make the above controller implementable, we have to introduce an approximation of the derivative operator (so called “*dirty derivative*” [8], which is given by a transfer function $\frac{s}{s/\tau+1}$, $\tau > 0$) for $\dot{\omega}$. Then the control law (19) is modified as follows:

$$\begin{aligned} T_{st} &= (1 - k\lambda_{cb}^{-1})\hat{T}_{cb} - \lambda_{cb}^{-1}(e - k\alpha - \dot{\alpha}) \\ \dot{\alpha} &= (2C_q r_g^3) \dot{\omega}_f - \lambda(\omega - \omega_d) \hat{\theta}_1 - \hat{\theta}_2 + \hat{\theta}_1 \lambda \dot{\omega}_d \\ \dot{\hat{T}}_{cb} &= -\lambda_{cb}(\hat{T}_{cb} - T_{st}) \\ \dot{\omega}_f &= \tau(\omega - \omega_f). \end{aligned} \quad (20)$$

With the approximation of the derivative, only semi-global practical stability results can be guaranteed, see the general procedure for deriving such results in [14].

7 Simulation Results

To illustrate the operation of the adaptive controller we have designed, we consider the response to a desired vehicle speed profile ω_d , given by a step-wise periodic function that may be encountered in typical urban driving scenarios. Initially, large parameter errors result in a poor tracking performance. The tracking improves as the adaptation proceeds. During this particular periodic excitation in ω_d the vehicle mass and road grade estimates tend to their true values in 45 sec as shown in Figure 5. From Figure 4 we note that v_{cb} saturates during the transients (the saturation limits are indicated by dash-dotted lines). To provide some compensation for saturation we use an approach from [15]. The idea is to replace ω_d by $\omega_{d,f}$ where $\dot{\omega}_{d,f} = -\lambda_f(\omega_{d,f} - \omega_d) + r$, where λ_f is large and r is selected to preserve the value of \dot{V}_d when saturation occurs and it is zero if there is no saturation. Unlike in [15], the scheme is here applied to an adaptive system. In particular, the saturation compensation scheme is active during the last downward step in ω_d (see Figure 3) and one can observe that the virtual reference $\omega_{d,f}$ slows down to enable the system to catch up with it. The controller scheme including the reference modification performed well for all the driving scenarios we tested through simulations. The analysis of the closed-loop stability properties for this more complex application is left for future work.

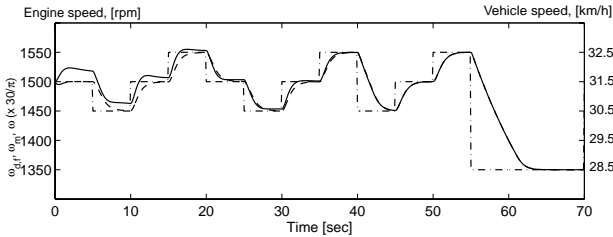


Figure 3: Vehicle speed ω (solid) in response to desired speed $\omega_{d,f}$ (dash-dot) and reference model trajectory ω_m (dash).

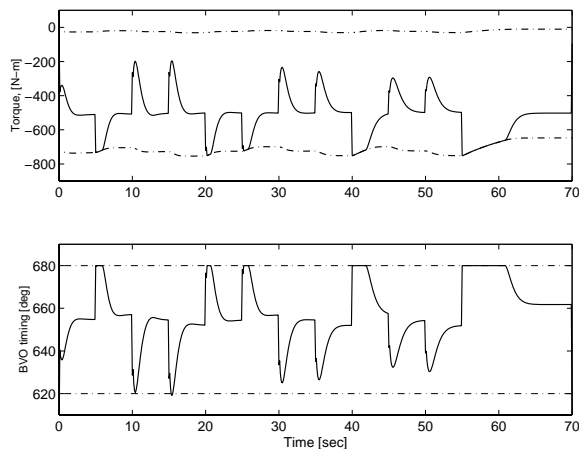


Figure 4: The trajectories of torque T_{st} and BVO timing v_{cb} (solid). $T_{st,max}$, $T_{st,min}$ and $v_{cb,max}$, $v_{cb,min}$ are indicated by dash-dotted lines.

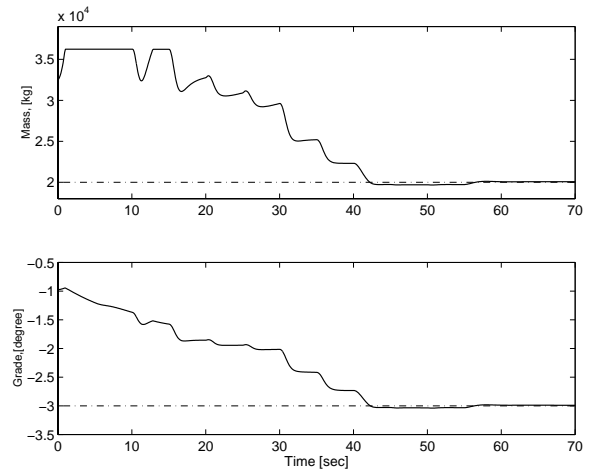


Figure 5: Convergence of vehicle mass and road grade parameter estimates. The true values are given by the dash-dotted lines, the estimates by the solid lines.

References

- [1] S.E. Shladover *et al.*, "Automatic vehicle control developments in the PATH Program," *IEEE Trans. on Vehicular Technology*, Vol. 40(1), 1991, pp.114-130.
- [2] P. Ioannou, C.C. Chien, "Autonomous intelligent cruise control", *IEEE Trans. on Vehicular Technology*, Vol. 42, 1993, pp.657-672.
- [3] C. Chen and M. Tomizuka, "Steering and independent braking control for tractor-semitrailer vehicles in automated highway systems," *Proceedings of the 34th CDC*, 1995.
- [4] D.D. Cummins, "The Jacobs engine brake application and performance", SAE Paper No. 660740.
- [5] Jacobs Vehicle System, "Intebrake engine braking system for Signature 600", retrieved on <http://www.jakebrake.com/products/engine>, March 1999.
- [6] H. Hu, M.A. Israel, and J.M. Vorih, "Variable valve actuation and diesel engine retarding performance," SAE Paper No. 970342.
- [7] D. Yanakiev and I. Kanellakopoulos, "Speed tracking and vehicle follower control design for Heavy-Duty Vehicles," *Vehicle System Dynamics*, Vol. 25, 1996, pp. 251-276.
- [8] D. Yanakiev and I. Kanellakopoulos, "Longitudinal control of automated CHVs with significant actuator delays," *Proceedings of the 36th CDC*, San Diego, 1997, pp. 4756-4763.
- [9] A.L. Fradkov, A.Yu. Pogromsky, *Introduction to Control of Oscillations and Chaos*, World Scientific, 1999.
- [10] L. Moklegaard, A. Stefanopoulou, J. Schmidt, "Transition from combustion to variable compression braking," SAE Congress, 2000-1-1228.
- [11] L. Moklegaard, A. Stefanopoulou, M. Druzhinina, "Brake valve timing and fuel injection: a unified engine torque actuator for Heavy-Duty Vehicles," submitted to AVEC'2000.
- [12] M. Krstic, I. Kanellakopoulos and P.Kokotovic, *Nonlinear and Adaptive Control Design*, Wiley, 1995.
- [13] P. Ioannou, J. Sun, *Robust Adaptive Control*, Prentice, 1996.
- [14] D. Swaroop, J.C. Gerdes, P.P. Yip and J.K. Hedrick, "Dynamic surface control of nonlinear systems," *Proceedings of the American Control Conference*, 1997, pp. 3028-3034.
- [15] J.-M. Kang and J.W. Grizzle, "Dynamic control of a SI engine with variable intake valve timing," *Proceedings of the 39th CDC*, 1999.